

Wireless Sensor Networks Powered by Ambient Energy Harvesting: An Empirical Characterization

Zhi Ang Eu*, Hwee-Pink Tan[†] and Winston K. G. Seah[‡]

*NUS Graduate School for Integrative Sciences and Engineering, National University of Singapore

[†]Networking Protocols Department, Institute for Infocomm Research (I²R), A*STAR, Singapore

[‡]School of Engineering and Computer Science, Victoria University of Wellington, New Zealand

Email: {euzhiang@nus.edu.sg, hptan@i2r.a-star.edu.sg and Winston.Seah@ecs.vuw.ac.nz}

Abstract—Wireless Sensor Networks Powered by Ambient Energy Harvesting (WSN-HEAP) can perform the task of continuous and remote monitoring of the environment without the need for replacement of batteries. We identify three important design considerations for wireless networking protocols in WSN-HEAP: the unpredictable energy supply, the propagation losses in different environments and the suitable power level to use. In this paper, we perform an empirical characterization of commercially available solar and thermal energy harvesting sensor nodes. We deploy a transmitter-receiver pair at different distances and in various environments to conduct link measurements to determine the packet delivery ratio and RSSI values. We also quantified the energy harvesting characteristics of the sensor node. Then, we analyze the collected data to provide insights and guidelines for designing networking protocols for WSN-HEAP. Our analysis shows that the transmission range of the node is highly dependent on the environment in which it is deployed in and the RSSI values can only be used to estimate the transmitter-receiver distance in some environments. Furthermore, the charging time exhibits large variances even in the absence of mobility.

I. INTRODUCTION

Traditional wireless sensor nodes use the stored energy in non-rechargeable batteries to operate. A sensor node is useless without energy, therefore research efforts have mainly focused on methods to maximize the lifetime of wireless sensor networks (WSNs) by reducing energy consumption. Recent research efforts have also focused on using harvested energy from the environment to power the sensor nodes. Due to the availability of different natural sources of ambient energy, energy harvesting is an attractive alternative to using non-renewable energy sources such as batteries. Using energy storage devices such as capacitors, supercapacitors or thin-film EnerChips to store the harvested energy, it is now possible to power a WSN using solely energy harvesting devices without the use of non-rechargeable batteries. The operating characteristics of a battery-operated WSN versus energy harvesting nodes are illustrated in Fig. 1a. For the rest of this paper, we use WSN-HEAP as the acronym for *Wireless Sensor Networks Powered by Ambient Energy Harvesting*.

In WSN-HEAP, each sensor node is equipped with a microcontroller, a radio transceiver for communication, one or more energy harvesting devices, an energy storage device to store the harvested energy and a sensor. The main hardware differences between a battery-operated and a WSN-HEAP node is illustrated in Fig. 2.

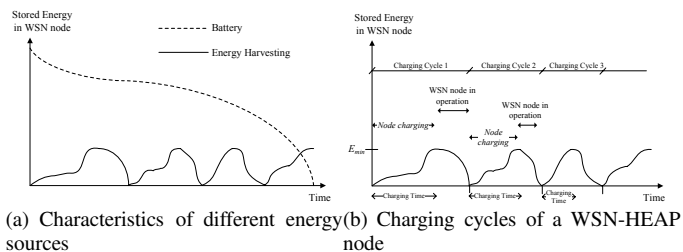


Fig. 1. Energy Characteristics of a WSN-HEAP node

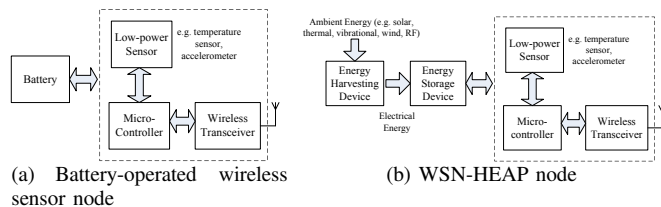


Fig. 2. Battery-operated versus energy-harvesting sensor node

One of the possible applications for WSN-HEAP is structural health monitoring (SHM). The current approach to SHM relies on wiring sensors mounted on structures to be monitored to data loggers. However, WSNs are increasingly being considered in SHM ([1],[2]). WSNs for SHM should be environmentally-friendly (without the use of batteries) and operate for very long periods of time (years or even decades). In some cases, it may be infeasible (with sensors embedded into structures in buildings) or hazardous (with sensors welded into structures at construction sites) to replace the batteries. Therefore, WSN-HEAP is suitable for SHM because no battery needs to be replaced. Other than monitoring buildings, energy harvesting wireless sensors have also been developed for monitoring the structures of aircraft [3].

In order to design networking protocols for practical deployment of WSN-HEAP, we empirically characterize the (i) radio behavior and (ii) charging times of commercially-available WSN-HEAP nodes in time and space. We consider solar and thermal energy harvesting nodes that use the MSP430 microcontroller and CC2500 radio transceiver from Texas Instruments (TI), as shown in Fig. 3.

This paper is organized as follows: In Section II, we review some work on energy harvesting technologies and their

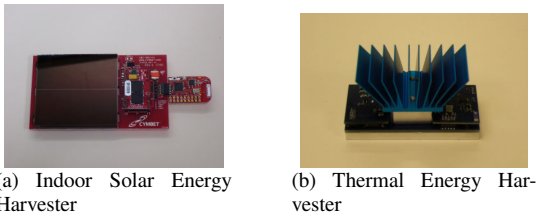


Fig. 3. Energy harvesting sensor nodes using MSP430 microcontroller and CC2500 transceiver from Texas Instruments

applications in wireless sensor networks. Next, we describe the experimental setup in Section III. Then, we present and discuss the measurement results in Section IV. We conclude the paper and outline our future work in Section V.

II. RELATED WORK

There are many commercial energy harvesting sensor nodes available. Ambiosystems [4] produces battery-less sensor nodes that can be powered by many types of energy harvesters. The sensor nodes developed by Microstrain [5] harvest energy from solar cells and piezoelectric materials. EnOcean [6] produces transmitters that can power themselves by harvesting ambient energy from the environment while Advanced Cerametrics [7] produces vibration-based energy harvesters. However, most of the datasheets provided by these companies only describe the energy harvesting technology/mechanism as well as the average harvesting rate but not the energy charging characteristics which are important in the design of networking protocols. Important energy charging characteristics include charging time and the number of packets that can be transmitted per charge cycle. While there have been many link measurement studies with the MICAz sensor node (e.g. [8]) or the TelosB sensor node (e.g. [9]), to the best of our knowledge, this is the first radio behavior study of the new CC2500 radio transceiver using an on-board antenna.

III. EXPERIMENTAL SETUP

A. WSN-HEAP Node

The sensor node development kit [10] we use consists of a solar panel optimized for indoor use, two eZ430-RF2500T target boards and one AAA battery pack. The kit is also widely used by many manufacturers including AdaptivEnergy, which manufactures vibrational energy harvesters. The target board comprises the TI MSP430 microcontroller, CC2500 radio transceiver and an on-board antenna. The CC2500 radio transceiver operates in the 2.4 GHz band with data rate of 250 kbps. It is designed for low power wireless applications and supports many transmit power levels (P_{tx}) as shown in Table I. The sensor node is powered using an energy harvester with the harvested energy being stored in a thin-film EnerChip manufactured by Cymbet. Compared to normal batteries, the thin-film EnerChip is rechargeable and has little self-discharge, making it suitable for use in a WSN-HEAP node. The thermal energy harvester is manufactured by Micropelt. The battery pack is mainly used for debugging application programs. In our experiments, the battery pack is also used for powering the

target board in the radio characterization tests. In addition to the development kit, we also use a TI evaluation board which acts as a sniffer to overhear packet transmissions by the TI sensor nodes in the energy measurement tests.

TABLE I
TRANSCIEVER CURRENT CONSUMPTION AT VARIOUS TRANSMIT POWER LEVELS

| Transmit Power, P_{tx} (dBm) | Current Consumption (mA) |
|--------------------------------|--------------------------|
| -30 | 9.9 |
| -28 | 9.7 |
| -26 | 10.2 |
| -24 | 10.1 |
| -22 | 10.0 |
| -20 | 10.1 |
| -18 | 11.7 |
| -16 | 10.8 |
| -14 | 12.2 |
| -12 | 11.1 |
| -10 | 12.2 |
| -8 | 14.1 |
| -6 | 15.0 |
| -4 | 16.2 |
| -2 | 17.7 |
| 0 | 21.2 |
| 1 | 21.5 |

For the link measurements, the transmitter uses power from the battery pack with the receiver directly connected to the computer as shown in Fig. 4a. For the energy measurements, the transmitter uses power from the energy harvesters as shown in Fig. 4b. The receiver in the energy measurements uses an evaluation board from TI instead of another sensor node because it provides more precise and accurate timings.

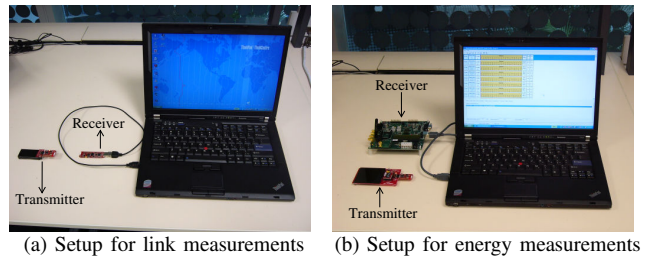


Fig. 4. Experimental setup

B. Characterization of Radio Behavior

The performance metrics we use to characterize the radio behavior are the packet delivery ratio (PDR) and RSSI. The PDR is defined as the ratio of the number of successful receptions out of 1000 packet transmissions. Each packet consists of 40 bytes of data with an additional 11 bytes of headers. If a packet can be correctly received by the receiver, the RSSI value for the packet is also recorded. We use a total of 17 transmit power levels as shown in Table I.

We carried out the radio characterization in four different environments. The anechoic chamber (Fig. 5a) and the open field (Fig. 5b) provide us with an obstacle-free indoor and outdoor environment respectively while the corridor (Fig. 5c) and the high-rise residential building (Fig. 5d) give us realistic

indoor and outdoor deployment environments respectively. For deployment in the building, we place the sensor nodes both horizontally and vertically apart to determine radio behavior under these two different placements. For horizontal placement (Fig. 6a), the sensor nodes are mounted onto beams. For vertical placement (Fig. 6b), the sensor nodes are placed across the ledges of each storey that are 2.5m apart from one another. The experimental setup in the different deployment sites are shown in Fig. 5 and the different transmitter-receiver distances (d_{tr}) are shown in Table II.

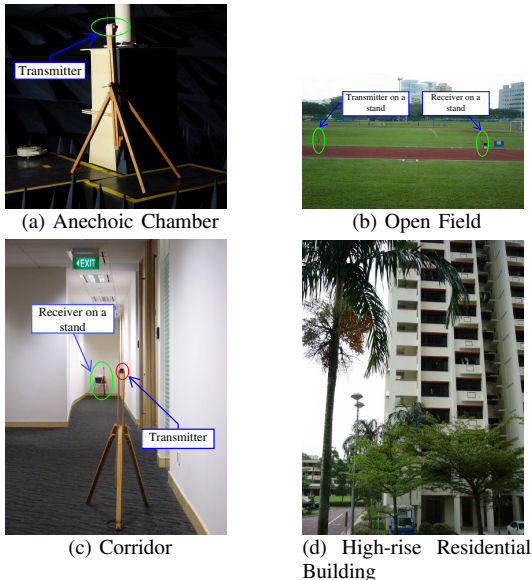


Fig. 5. Different deployment sites for link measurements

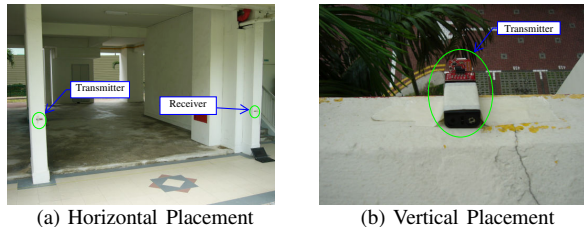


Fig. 6. Deployment of sensor nodes in high-rise residential building

TABLE II
TRANSMITTER-RECEIVER DISTANCES IN DIFFERENT ENVIRONMENTS

| Environment | Transmitter-receiver distance, d_{tr} (m) |
|-----------------------|---|
| Anechoic Chamber | 10, 12, 14 |
| Corridor | 2-30 in steps of 2 |
| Open Field | 4-80 in steps of 4 |
| Building (Horizontal) | 4.4, 7.4, 10.4, 14.6, 18, 22.3, 25.3 |
| Building (Vertical) | 2.5 to 12.5 in steps of 2.5 |

C. Energy Harvesting Characteristics

To quantify the energy harvesting characteristics, the transmitter is powered by solar or thermal energy harvesters in Fig. 3. After some *charging* time, when enough energy has been harvested and accumulated (E_{min} as shown in Fig.

1b) in the energy storage device, the power supply for the microcontroller and transceiver will be switched on. Then, the transmitter will continuously broadcast data packets until the energy is depleted after which the microcontroller and transceiver will be turned off. The energy storage device will start to accumulate energy again and the process is repeated in the next cycle as illustrated in Fig. 1b. We record the charging time as well as the number of packets transmitted for each cycle. The rate of energy harvesting depends on both the type and location of the energy harvester. For the solar energy harvester, we place it (i) directly under (Fig. 7a), (ii) on a table 1m under, and (iii) on a table 2m under a ceiling fluorescent lamp. For the thermal energy harvester, we place it on a CPU heat sink inside a computer (Fig. 7b) to model the harvesting of wasted heat energy from machinery.

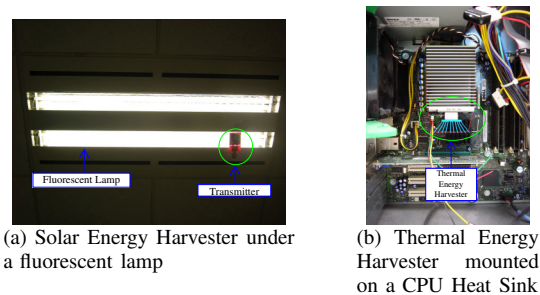


Fig. 7. Placement of energy harvesters for energy measurements

IV. MEASUREMENT RESULTS AND DISCUSSIONS

A. Packet Delivery Ratio

1) *Indoor Environments*: The PDR measurements for the anechoic chamber are shown in Fig. 8a. For clarity, if the PDR for a particular power level is 0 for all the transmitter-receiver distances in Table II, the plot for that power level is omitted from the graph. The results show that the individual plots of different power levels do not cross one another so a higher power level can always achieve a higher PDR up to the maximum of 1. Next, we consider the results for the corridor scenario as shown in Fig. 8b. Unlike the anechoic chamber, a lower power level can sometimes achieve a higher PDR than a higher power level.

2) *Outdoor environments*: The results for the open field are shown in Fig. 8c. At each fixed distance d_{tr} , a higher power level can achieve a higher PDR. However, for different transmitter-receiver distances, sometimes the PDR for a shorter distance is lower than the PDR for a longer distance. Finally, the results for horizontal and vertical placement for the residential building are shown in Figs. 8d and 8e respectively. We observe that the PDR for horizontal placement is much higher than that for vertical placement.

3) *Comparison between indoor and outdoor environments*: Fig. 8f compares the PDR under different environments using the highest transmission power of 1 dBm. We can observe that the node has a maximum transmission range of about 70m in the open field with PDR above 0.5. Many commonly-used

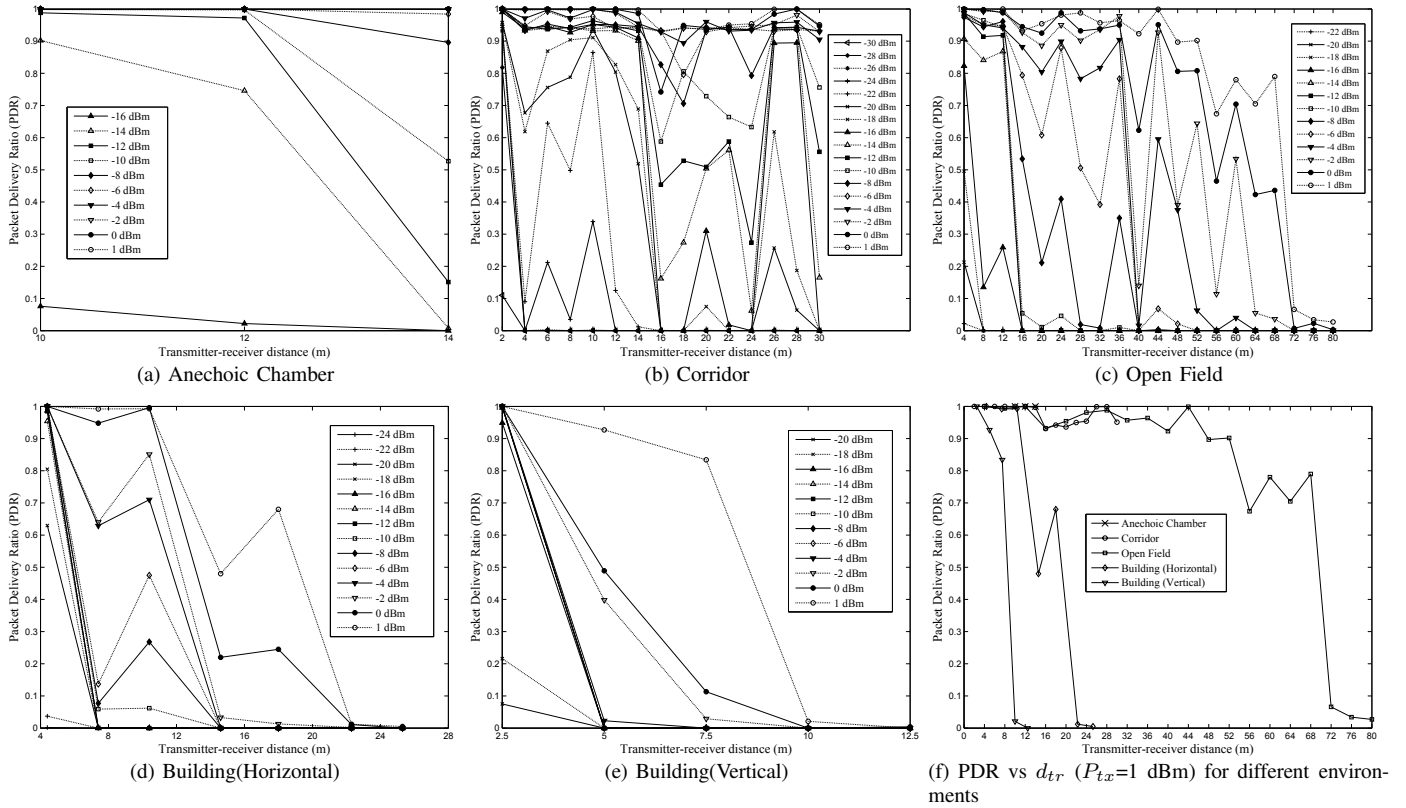


Fig. 8. Packet delivery ratio (PDR) under different environments and transmit power levels

or well-studied propagation models, including the freespace propagation model, have the following two properties: (i) For a fixed transmitter-receiver distance d_{tr} , increasing transmission power P_{tx} will increase PDR, and (ii) For a fixed transmission power P_{tx} , the PDR will decrease as the transmitter-receiver distance d_{tr} increases.

Table III summarizes whether the propagation characteristics in the different environments satisfy these two properties. This will provide useful design guidelines to engineers when deploying and using power control in WSN-HEAP. For example, increasing transmission power in an open environment (e.g. the open field) will almost always increase PDR but not so in an indoor environment (e.g. the corridor). Furthermore, this shows that theoretical or known propagation models do not always fit or apply in every environment due to multipath propagation as well as fading and shadowing effects, therefore empirical studies have to be done before deployment to optimize performance.

TABLE III
PROPAGATION CHARACTERISTICS IN DIFFERENT ENVIRONMENTS

| Environment | PDR increases as P_{tx} increases (fixed d_{tr}) | PDR decreases as d_{tr} increases (fixed P_{tx}) |
|-----------------------|---|---|
| Anechoic Chamber | Yes | Yes |
| Corridor | Not always | Not always |
| Open Field | Most of the time | Not always |
| Building (Horizontal) | Yes | Not always |
| Building (Vertical) | Yes | Yes |

B. Link Quality Measurements

Fig. 9 shows the RSSI values of the packets received under different environments using the highest P_{tx} value (1 dBm) versus d_{tr} . The average RSSI values and the corresponding 95% confidence levels are shown. In general, RSSI readings correlate with transmitter-receiver distances as RSSI values decrease (increase) when d_{tr} increases (decreases), therefore RSSI readings are often used in ranging or localization algorithms. In our tests, we find that RSSI readings correlate highly with transmitter-receiver distances in the anechoic chamber and building. The correlation decreases in the open field and is the least in the corridor environment.

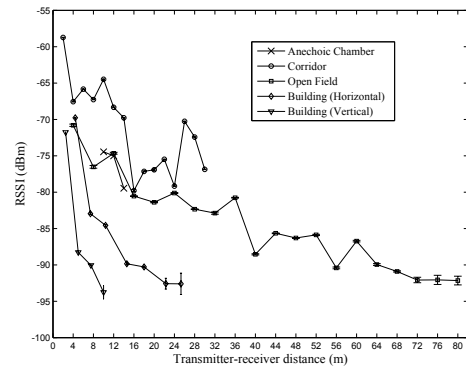


Fig. 9. Average RSSI values versus d_{tr} ($P_{tx}=1$ dBm)

C. Energy Measurements

First, we measure the number of packets that can be transmitted per charge cycle, and the results are shown in Fig. 10. The readings are averaged over 100 charge cycles and the corresponding 95% confidence levels are shown. In general, to transmit at higher transmission powers, more energy is required to transmit each packet and therefore less packets can be transmitted. However, from the datasheet provided by TI for the CC2500 transceiver and shown in Table I, for some power levels, it takes less energy to transmit at higher output powers. For example, the current consumption to transmit at -18 dBm is 11.7 mA while the current consumption to transmit at a higher transmit power of -16 dBm requires only 10.8 mA. This is also validated by our experiments where we can send an average of 26.8 and 28.9 packets per charge cycle at -18 dBm and -16 dBm respectively. This shows that -16 dBm may be a better choice than -18 dBm since we can send more packets with possibly longer transmission ranges and higher PDR with the -16 dBm transmission power.

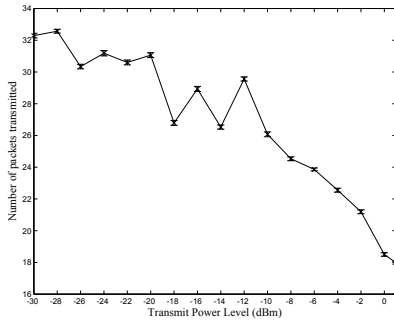


Fig. 10. Number of packets transmitted in each charge cycle

Figs. 11a, 11b and 11c illustrate the probability density functions (pdf) of the charging times for 1000 charge cycles when the solar energy harvester is placed directly under, 1m and 2m under the fluorescent lamp (scenarios 1, 2 and 3) respectively. The results show that there is greater variation (higher standard deviation) in the charging time required for each charge cycle when the sensor node is further away from the light source. The corresponding pdf for the thermal energy harvester on the CPU heat sink (scenario 4) is shown in Fig. 11d. The statistics for these scenarios are shown in Table IV. It can be observed that even without mobility, the energy harvesting times vary across charging cycles.

TABLE IV
CHARGING TIME STATISTICS

| | Scenario 1 | Scenario 2 | Scenario 3 | Scenario 4 |
|---------------------|------------|------------|-------------|------------|
| Minimum | 1208.63 ms | 4753.88 ms | 7470.19 ms | 1818.71 ms |
| Maximum | 1286.12 ms | 6734.70 ms | 12279.66 ms | 2422.81 ms |
| Average | 1266.10 ms | 5854.37 ms | 9655.25 ms | 1980.46 ms |
| Standard deviation | 8.12 ms | 340.34 ms | 623.37 ms | 105.14 ms |
| Bin size in Fig. 11 | 5 ms | 50 ms | 100 ms | 10 ms |

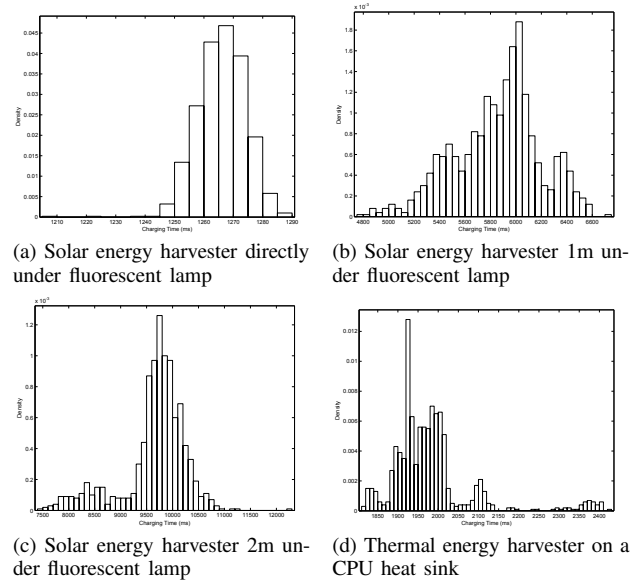


Fig. 11. Probability density functions of charging times in different scenarios

V. CONCLUSION AND FUTURE WORK

We have presented the important factors that affect wireless networking protocols for WSN-HEAP. Our findings show that compared to ideal conditions, there is significant signal attenuation when we deploy commercially available WSN-HEAP nodes in real world environments. These measurements have helped us improve our understanding of the propagation models of the latest TI sensor nodes in different environments, and they could provide useful guidelines to engineers in deploying such nodes. From our energy measurements, we find that the charging times vary in different scenarios and the number of transmitted packets per cycle depends on the transmit power. Based on the measurement results that we have collected, we are going to design energy efficient multihop MAC and routing algorithms for WSN-HEAP.

REFERENCES

- [1] G. Park, C. R. Farrar, M. D. Todd, W. Hodgkiss, and T. Rosing, "Energy Harvesting for Structural Health Monitoring Sensor Networks," Los Alamos National Laboratory, Tech. Rep., Feb. 2007.
- [2] N. Xu, S. Rangwala, K. K. Chintalapudi, D. Ganesan, A. Broad, R. Govindan, and D. Estrin, "A Wireless Sensor Network For Structural Monitoring," in *SenSys*, 2004, pp. 13–24.
- [3] S. W. Arms, J. H. Galbreath, C. P. Townsend, D. L. Churchill, B. Corneau, R. P. Ketcham, and N. Phan, "Energy Harvesting Wireless Sensors and Networked Timing Synchronization for Aircraft Structural Health Monitoring," in *Wireless VITAE*, 2009.
- [4] "Ambiosystems." [Online]. Available: <http://www.ambiosystems.com>
- [5] "Microstrain." [Online]. Available: <http://www.microstrain.com>
- [6] "EnOcean." [Online]. Available: <http://www.enocean.com>
- [7] "Advanced Cerametrics." [Online]. Available: <http://www.advancedcerametrics.com>
- [8] W. Su and M. Alzaghaf, "Channel propagation characteristics of wireless MICAZ sensor nodes," *Ad Hoc Networks*, vol. 7, no. 6, pp. 1183–1193, Aug. 2009.
- [9] R. Maheshwari, S. Jain, and S. R. Das, "A Measurement Study of Interference Modeling and Scheduling in Low-Power Wireless Networks," in *ACM SenSys*, 2008, pp. 141–154.
- [10] "MSP430 Solar Energy Harvesting Development Tool (eZ430-RF2500-SEH) from Texas Instruments." [Online]. Available: <http://www.ti.com>